Special Issue Article | ICADET 2017[C]

Turkish Journal of Electromechanics & Energy

ISSN-2547-975X

Single Input, Multiple Output DC-DC Buck Converter for Electric Vehicles

İlyass Abdillahi Aden [1*], Hakan Kahveci[1], Mustafa Ergin Şahin[2]

[1]Karadeniz Technical University, Department of Electrical and Electronics Engineering, Trabzon, 61080, Turkey
[2]Recep Tayyip Erdoğan University, Department of Electrical and Electronics Engineering, Rize, 53100, Turkey

Received: 14 November 2017; Revised 14 December 2017 Accepted: 15 December 2017; Published: 30 December 2017
Academic Editor: H. İ. Okumuş
Turk J Electrom Energ Vol.: 2 No: 2 Page: 7-13 (2017)
SLOI: http://www.sloi.org/
*Correspondance E-mail: ilyaden1992@gmail.com

ABSTRACT Increasing concerns on environmental pollution, global warming, depletion of the fossil fuel reserves and desire for reducing energy dependencies have led to an ever-increasing interest in electric vehicles (EV). The requirements for electric vehicles has brought many different problems and solutions in electric vehicle technology. One of these is the conversion of the voltage level from the battery in electric vehicles to other required voltage levels with DC-DC converters. As a solution, a separate converter can be used for each voltage level. Nevertheless, single-input multi-output (SIMO) converters can be used to reduce the cost and switching losses and hence improve system efficiency. In our study, we proposed non-isolated buck converter topology with single-input (48 V) and multi-output (12 V and 5 V). The 12 V voltage level is used for the horn, headlights while 5 V voltage level is used for the telemetry and microcontroller in electric vehicles. In this work, the general structure of a SIMO converter, design principles, small signal and stability analysis, and control steps are explained. The overall system has been simulated with Matlab / Simulink.

Keywords: Electric Vehicles, DC-DC Buck Converter, Single Input Multiple Output, Steady State Analyses, PI controller, Matlab/Simulink

Cite this article: İ. A. Aden, H. Kahveci, M. E. Şahin, Single Input, Multiple Output DC-DC Buck Converter for Electric Vehicles, Turkish Journal of Electromechanics & Energy 2(2) 7-13 (2017)

1. INTRODUCTION

Increasing demand for energy in the world and the diminishing of fossil energy sources promotes exploitation of other energy sources such as solar energy, fuel cells and other clean energy sources. These energies are usually environmentally friendly [1]. The primary utilizations of DC–DC converters include uninterruptible power supplies, battery charging/discharging devices, hybrid electric vehicle, and renewable energy systems [2-7]. Occasionally, in a typical buck converter, an active power switch replace the freewheeling diode [8–12]. A single input multiple-output DC–DC converter able of providing, boost, buck and inverted outputs at the same time has been presented in literature [13]. However, three switches are required for one output. This type of designs correspond only for low power application and output voltage. Multi-output DC–DC boost converter are studied in an another study [14]. Output voltage for high and low power applications is shared in this study. Nevertheless, for one output voltage two switches were required and its control scheme is complicated. Kumar and Omar present Single-Input Multiple-Output (SIMO) Synchronous DC-DC buck converter [15]. It has advantage of reducing the number of the switches; four switches are required for over three output voltage. Unfortunately, this SIMO converter has the disadvantage of requiring a higher current rating for four switches. Another single input, multiple outputs DC-DC converter has been proposed by Kwon, and Mora [16]. This converter is capable of providing both boost and inverted outputs. Nonetheless, in this new configuration, the loads are separately designed except the negative output. Double-output DC-DC buck converters with unidirectional and bidirectional characteristics has been presented by Santos [17]. However, the buck converter required power switches with high current ratings.

[C]*Initial version of this paper was selected from the proceedings of International Conference on Advanced Engineering Technologies (ICADET 2017) which was held in September 21-23, 2017, in Bayburt, TURKEY; and was subjected to peer-review process prior to its publication.*

This paper presents a bi-directional SIMO DC-DC buck converter for electric vehicles battery as shown in the Figure 1. The main aim of this converter is to buck the voltage coming from the battery to the different components. The presented topology has the advantage of having three switches for two outputs. In addition, the control strategies, design principles, and small signal analysis has been included. The system has been simulated in MATLAB/Simulink.

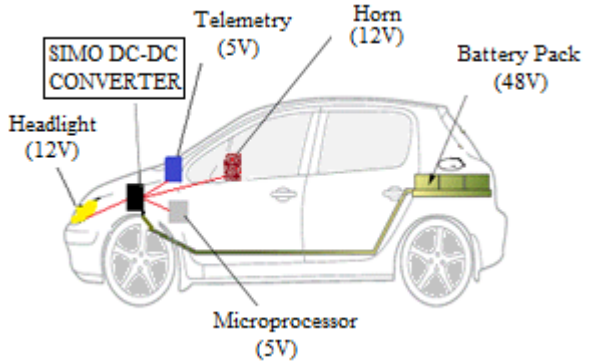

Fig. 1. SIMO DC-DC converter in electric vehicles

2. BUCK AND SIMO CONVERTER TOPOLOGY

2.1. Buck Converter

Buck converter is a step-down DC-to-DC converter, where the output voltage is lower than the input voltage [19]. The basic buck converter circuit is presented in Figure 2.

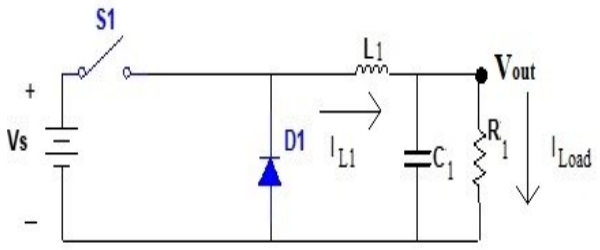

Fig. 2. Basic buck converter circuit

For the converter shown above, the current flows across the inductor in to the load when the switch (S_1) is closed. This current charges the inductor (L_1) by boosting both its magnetic field and voltage output. After a while, the output voltage (V_{out}) will attain the desired value; then the switch (S_1) is turned off and the current flows through the recovery diode (D_1). At this state, inductor (L_1) is discharged and current continues to flow through it. Before the inductor is fully discharged, the S_1 is turned on, D_1 is turned off and the cycle repeats. One can settle the ratio between the input and output voltage by modifying the duty cycle of the switch (S_1).

2.2. SIMO Converter

Single input, multiple output topology that is used in this study is given in Figure 3.b. The bi-directional DC-DC converter used in this paper has less power loss distribution among the power switches than unidirectional characteristics [12]. The topology consists of three power switches S_1; S_2 and S_3 as well as two low pass filters (L_1-C_1 and L_2- C_2) as illustrated in Figure 3.b. The state of the switches is represented as *switch x* = OFF (0) and *switch x* = ON. Since there are three switches and two states for each switch, we obtain eight ways of operating of the presented converter [11]. Three switching states are operational, only. The other combinations were not included in this work. Table I presents the topological states (TS) of the system designed.

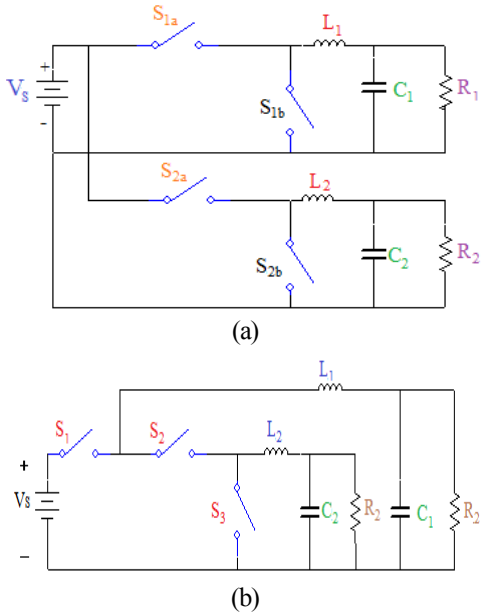

Fig. 3. Bi-directional SIMO DC-DC buck converter: (a) Parallel solution, (b) Implemented solution

The different switching states of SIMO converter are shown in Figure 4. It can be observed from the Figure 4 that:

-*In state TS-1:* Switch 1 = 1, Switch 2 = 1 and Switch 3 = 0. The input voltage (V_s) supplies energy to the loads and to the inductors, in this state both L_1 as well as L_2 is charged.

- *In state TS-2*: Switch 1 = 1, Switch 2 = 0 and Switch 3 =1. The input voltage (V_s) supplies energy to R_1–L_1 and current of the inductor L_2 (i_{L2}) flows across S_2, delivering some of its energy to the load R_2. In this circumstance, inductance L_1 and L_2 will be respectively charged and discharged.

- *In state TS-3*: Switch 1 = 0, Switch 2 = 1 and Switch 3 =1. The current in the inductor L_1 (i_{L1}) flows to both S_2 and S_3, while i_{L2} flows only across S_3, delivering its stored energy to both loads R_1 and R_2. In this situation the inductor L_1, as well as the inductor L_2 are discharged.

Table 1. Topological states of the used SIMO converter

Topological states	TS-1	TS-2	TS-3
Switch 1	ON	ON	OFF
Switch 2	ON	OFF	ON
Switch 3	OFF	ON	ON

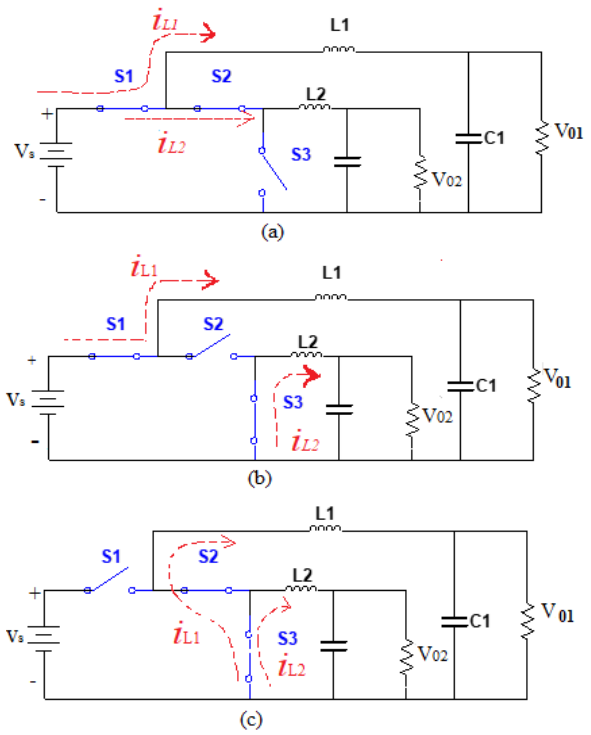

Fig. 4. The different switching states of the SIMO converter: (a) TS-1, (b) TS-2, (c) TS-3

3. STEADY STATE ANALYSIS

The presented SIMO converter is devised to operate in continuous conduction mode (CCM). The current and voltage waveforms of inductors are presented in Figure 5. T_{ON1} and T_{ON2} are the periods which the PWM generators one and two are generating the logic "1" at their corresponding outputs.

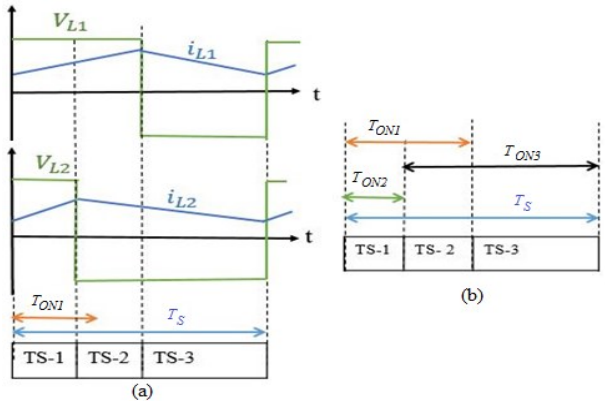

Fig. 5. Steady-state analysis of the SIMO converter; (a) Inductors current and voltage related with topological states, (b) Times in which the switch S_1, S_2 and S_3 are turned ON.

From the topological states and waveforms found in the foregoing section, it can be inferred that the output voltage V_{01} and V_{02} controls voltage V_{R1} and V_{R2} respectively. Noting that the average inductor voltage is zero, the following equations are written:

$$(V_S - V_{01}) * T_{ON1} = V_{01} * (T_S - T_{ON1}) \quad (1)$$

$$(V_S - V_{02}) * (T_S - T_{ON3}) = V_{02} * T_{ON3} \quad (2)$$

According to the equations (1, 2), the different output voltages come out as a function of their input voltage and duty cycles. V_{01} and V_{02} are expressed in the following equations:

$$V_{01} = (D_1)V_S \quad (3)$$

$$V_{02} = (1 - D_2)V_S \quad (4)$$

where D_1 and D_2 represent the duty cycles of the system.

4. GENERALIZED STATE-SPACE AVERAGE MODEL

The voltage and the current dynamics are described by the state space average and it is given in (5)-(8):

$$L_1 \frac{di_{L1}}{dt} + Vo_1 = D_1 Vs \quad (5)$$

$$C_1 \frac{dV_{01}}{dt} = i_{L1} - \frac{V_{01}}{R_1} \quad (6)$$

$$L_2 \frac{di_{l2}}{dt} + Vo_2 = D_2 Vs \quad (7)$$

$$C_2 \frac{dV_{02}}{dt} = i_{L2} - \frac{V_{02}}{R_2} \quad (8)$$

By using these equations and the state equation, the transfer functions obtained between the output voltages and the duty ratios are as follows:

$$Tp_1(s) = \frac{V_S D_1 R_1}{(R_1 C_1 L_1 s^2 + L_1 s + R_1)} \quad (9)$$

$$Tp_2(s) = \frac{V_S D_2 R_2}{(R_2 C_2 L_2 s^2 + L_2 s + R_2)} \quad (10)$$

The circuit component's values are calculated as follow:
- Output 1: For P_1= 150W/12V, V_S=48, R_1=1Ω, L_1=180µF, C_1=20µF.
- Output 2: For P_2= 25W/5V, V_S=48, R_2 =1Ω, L_2=89µF, C_2=62µF.

In the open loop the circuit transfer function with their numerical values are found as follows:

$$Tp_1(s) = \frac{12}{(3.6*10^{-9}s^2 + 180*10^{-6}s + 1)} \quad (11)$$

$$Tp_2(s) = \frac{5}{(5.5*10^{-9}s^2 + 62*10^{-6}s + 1)} \quad (12)$$

5. SIMULATION AND RESULTS

5.1. Simulink Model of SIMO DC-to-DC Converter

The simulation model of the whole system is shown in Figure 6. The system is composed of two PWM block, one logic block and the SIMO converter. The input voltage of the converter is 48 volt and the output is composed of 5 and 12 volts.

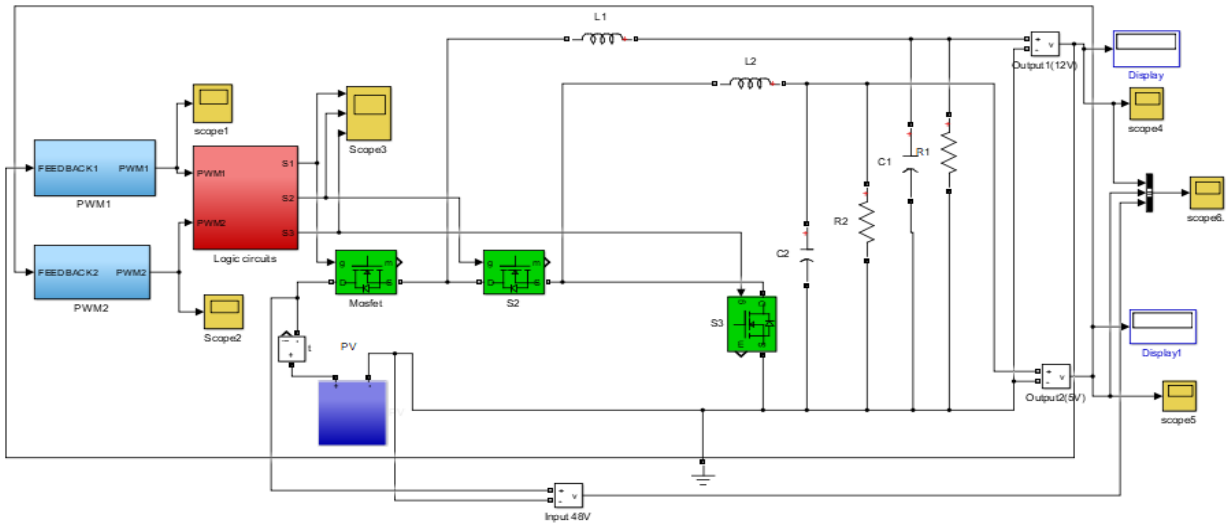

Fig. 6. Simulink diagram of the SIMO DC-DC converter

5.1.1. PWM Generator Implementation and PI Controller

All three switches discussed are controlled using PWM, and this block include PI controller. The Simulink model is given in Figure 7. DC-to-DC converters use switches to change the DC from one level to another [20]. The system operates at 50 kHz with an output value between 0 and 1. The PWM1 and PWM2 generators produce an error signal and inserted into the PI block. The output of the PI block is compared to the sawtooth. Thus, logic 1 and 0 values are produced. The PI controller is a proportional-integral controller. In our case, we used PI to control the output voltage coming from the SIMO DC-DC buck converter [18, 21]. The values of the gains K_P, and K_I, are chosen carefully using Routh–Hurwitz stability criterion. The output would reach the reference value with a very short settling time and without an overshoot.

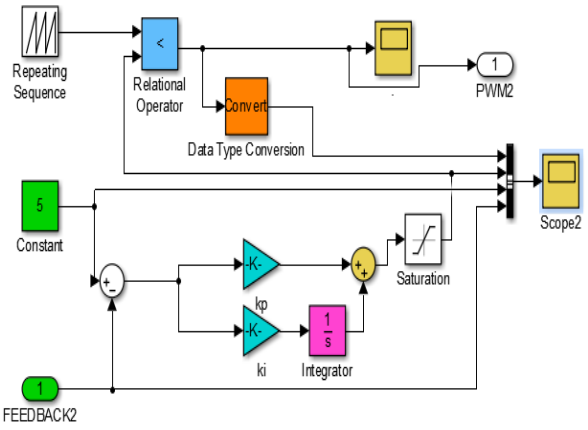

Fig. 7. PWM and PI design with Matlab/Simulink

5.1.2 Modelling the Logic Circuits

The outputs of the PWM1 and PWM2 which is illustrated in Figure 7 straightly go through a logic circuit (LC) block as given in Figure 6. This LC block command the state of the switches S_1, S_2 and S_3. From the topological states point of view (shown in Table I), it can be deduced that the charging of the inductor L_1 is fully reliant to switch 1 (S_1), consequently to control V_{O1} the PWM1 is directly connected to S_1. In contrary, either charging or discharging of L_2 is not reliant on the state of S_2 since when the L_2 is discharging in the TS-3 the switch S_2 is ON. The second PWM generator defines an interval that the switch S2 should begin to operate. In addition, switch S_2 should be controlled in such a way that prohibited states are avoided. These requirements are achieved by using a two input "OR" gate and a "NOT" gate shown. Lastly, the other two switches specify the switch S3. This deduces that the only work for the switch S_3 to avoid the prohibited states. This is achieved using NAND gate. The logic block is shown in Figure 8(a) and the gate signals of S_1, S_2 and S_3 are presented in Figure 8(b).

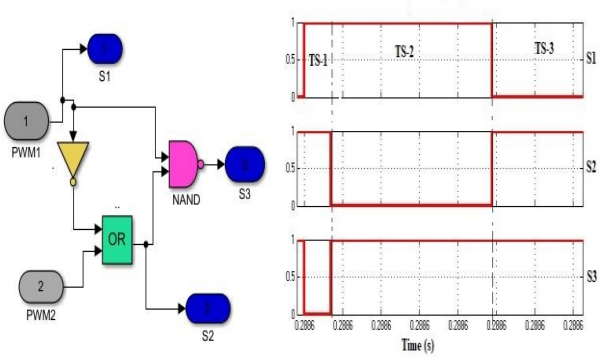

(a) (b)

Fig. 8. Gate signals of the switches: (a) Logic block; (b) Output signals of the block

5.2. *SIMO DC-DC Converter Represented with Transfer Function*

The simulation diagram of single input, multiple output (SIMO) converter along with transfer function presented in this paper and the results are shown respectively in Figures (9, 10).

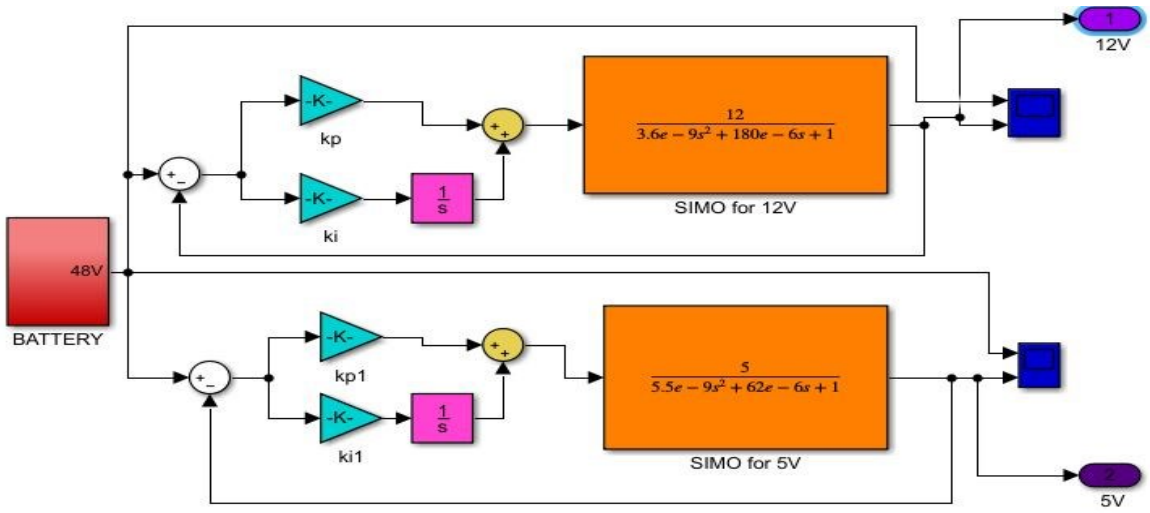

Fig. 9. SIMO converter with transfer function diagram

Figure 10 shows the simulation results of the transfer function of DC-DC converter. It can be deduced that all outputs reach their values in short time.

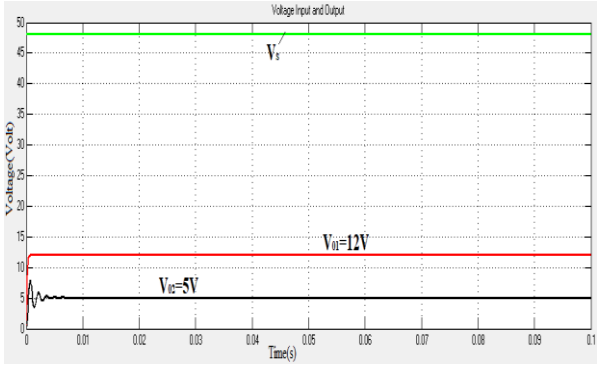

Fig. 10. The SIMO DC-DC converter

The PI controller continuously detect an error signal as the difference between feedback loop and the reference voltage. During the first zone, the feedback signal (black line) is less than the reference value (green line) as seen in the Figure 11, so error is negative. The PI controller produces signal (red color line) to eliminate the difference between feedback and reference and the switch S_1 is ON. During this period, the PWM generate pulses. In the second section, the feedback is higher than reference of 12 V, so error is positive. The PI is not generating a signal and the switch S_1 is OFF.

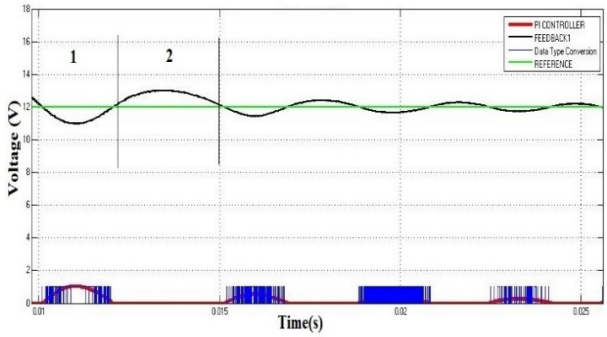

Fig. 11. Working principle of PI controller designed with Matlab/Simulink

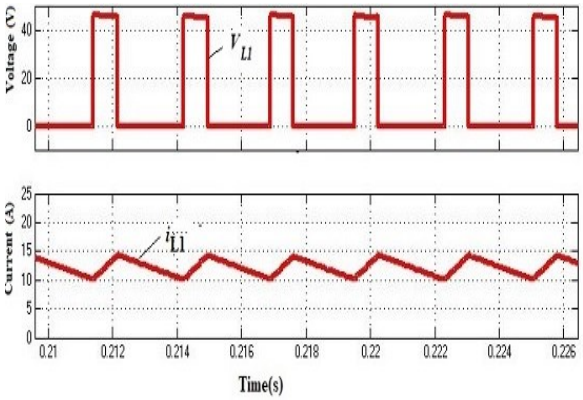

(a)

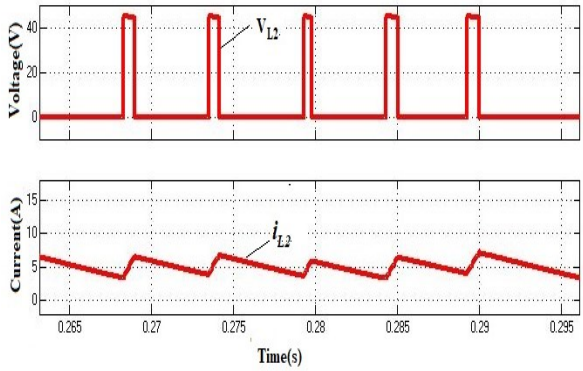

(b)

Fig. 12. Voltage and current associated with each inductor: (a) Variables of the inductor L_1, (b) Variables of the inductor L_2

The Simulink model of the SIMO DC-DC converter is given in Figure 13. Adding that all the required output voltages reaches their values with a very small overshoot.

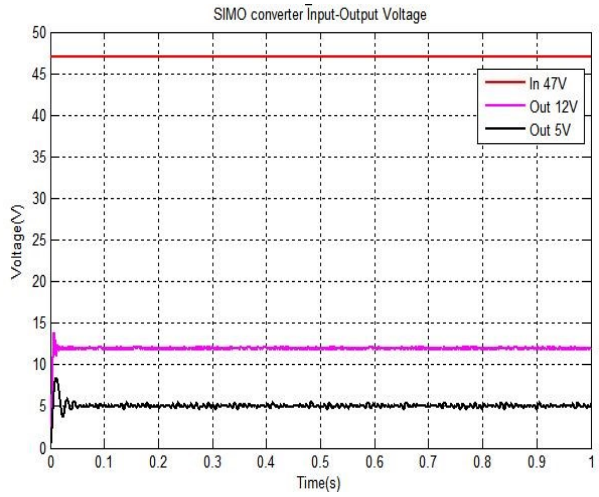

Fig. 13. Input and output voltages of SIMO DC-DC converter

Current in the load R_1 and R_2 is shown respectively in Figure 14 (a, b) when both loads are equal to 1Ω. When load is increased to R_1= R_2 =1.5 Ω, one can observe that the output current decrease as shown in Figure 15 (a, b). This implies that the output currents depend on the load. When the load is increased, the current decreases. The same when the load decreases, the current increases.

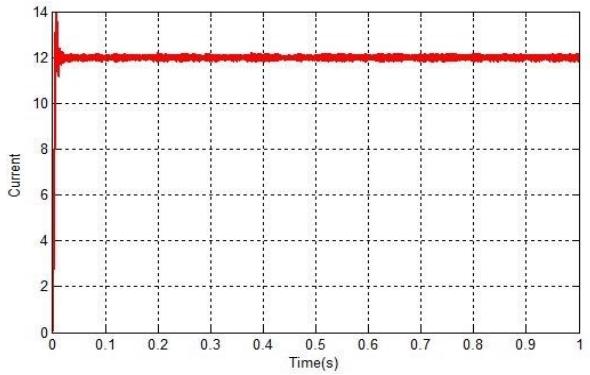

(a)

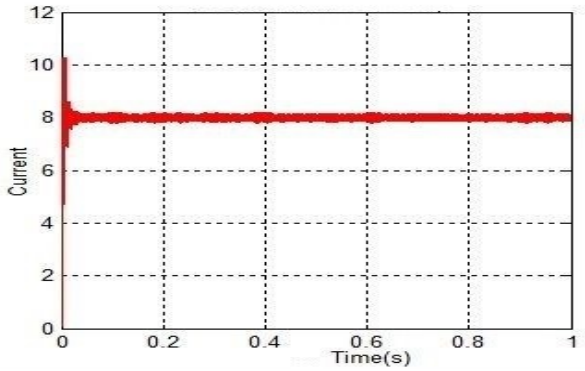

(b)

Fig. 14. The current as a function of loads: (a) Load R_1=1 Ω (b), Load R_2=1 Ω

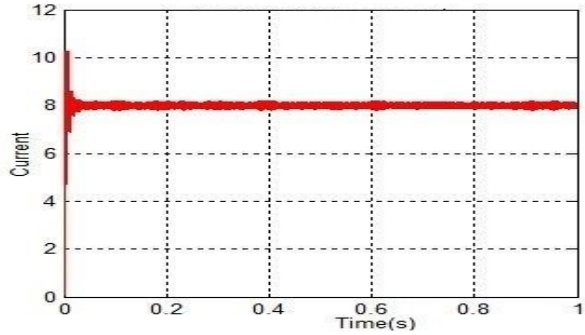

(a)

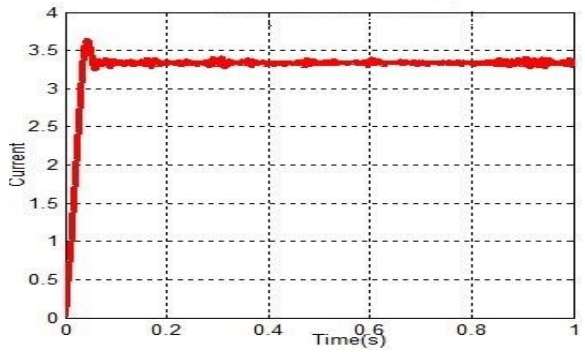

(b)

Fig. 15. The current as a function of loads: (a) Load R_1=1.5 Ω (b), Load R_2=1.5 Ω

6. CONCLUSION

In this study, we have used single-input, multiple-output converter that can be used for electric vehicles. Steady state analysis of the models, control strategies and PWM implementations are presented. The simulation of the both dynamic model and static model is performed in Matlab/Simulink. Simulink results show that this converter is suitable for the electrical vehicles. The idea of using only one converter that can supply power for different voltage output requirements is not far away. Efforts continue to realize single-input multiple-output buck converter more efficient in their control schemes and cost-effective for the integration of electric vehicles, renewable energy systems, mobile equipments, batteries and other applications.

References

[1] P. U. Sanchis, and L. Marroyo, Adaptive voltage control of the DC/DC boost stage in PV converters with small input capacitor, IEEE Trans. Power Electron., 28(11), 5038–5048, (2013).

[2] D. G. Chatterjee, and B. Fernandez, Modified soft-switched three-phase three-level DC–DC converter for high-power applications having extended duty cycle range, IEEE Trans. Ind. Electron., 59(9), 3362–3372, (2012).

[3] N. M. L. Tan, T. Abe, and H. Akagi, Design and performance of a bidirectional isolated DC–DC converter for a battery energy storage system, IEEE Trans. Power Electron., 27(2), 1237–1248, (2012).

[4] Z. Ouyang., Z. Zhang, O. C. Thomsen, and M.A.E Andersen, Planar-integrated magnetics (PIM) module in hybrid bidirectional DC–DC converter for fuel cell application, *IEEE* Trans. Power Electron. 26, (11), 3254–3264, (2011).

[5] Z. Zhang, Z. Ouyang, O.C. Thomsen, and M.A.E. Andersen, Analysis and design of a bidirectional isolated DC–DC converter for fuel cells and supercapacitors hybrid system, IEEE Trans. Power Electron, 27(2), 848–859, (2012).
[6] K. J. Ruan, K. Yang, and M. Xu, Power management for fuel cell power system cold start, IEEE Trans. Power Electron., 24(10), 2391–2395, (2009).
[7] L. Wang, Z. Wang, and H. Li, Asymmetrical duty cycle control and decoupled power flow design of a three-port bidirectional DC–DC converter for fuel cell vehicle application, IEEE Trans. Power Electron, 27(2), 891–904, (2012).
[8] V. A. Babazadeh, B. Ramachandran, L. Pao, D. Maksimovic, and E. Alarcon, Proximate time optimal digital control for synchronous buck dc-dc converters, IEEE Transaction on Power Electronics, 23(4), 2018–2026, (2008).
[9] F. Lee, K. Yao, M. Xu, and M. Ye, Tapped-inductor buck converter for high-step-down DC-DC conversion, IEEE Transaction on Power Electronics, 20, 775–780, (2005).
[10] D. Maksimovic, and X. Zhang, Multimode digital controller for synchronous buck converters operating over wide ranges of input voltages and load currents, IEEE Transaction on Power Electronics, 25(8), 1958–965, (2010).
[11] K. Yao, Y. Qiu, M. Xu, and F. Lee, A novel winding coupled buck converter for high frequency, high-stepdown dc-dc conversion, IEEE Transaction on Power Electronics, 20, 1017–1024, (2005).
[12] Y. Y. Mai, and P. Mok, A constant frequency output ripple-voltage-based buck converter without using large ESR capacitor, IEEE Trans. Circuits and Systems II, 55, 748–752, (2008).
[13] P. Patra, A. Patra, and N. Misra, A single inductor multiple output switcher with simultaneous buck, boost, and inverted outputs, IEEE Trans. Power Electron., 27(4), 1936–1951, (2012).
[14] A. Nami, F. Zare, A. Ghosh, and F. Blaabjerg, Multiple-output DC–DC converters based on diode-clamped converters configuration: Topology and control strategy, IET Power Electron., 3(2), 197–208, (2010).
[15] B. K. Sabbarapu, O. Nezamuddin, A. McGinnis, and E. dos Santos. Single-input multiple-output synchronous DC-DC buck converter, IEEE Energy Conversion Congress and Exposition (ECCE), (2016).
[16] D. Kwon, and G. A. R. Mora, Single-Inductor–Multiple-Output Switching DC–DC Converters, IEEE transactions on circuits and systems—ii: express briefs, 56(8), (2009).
[17] E. C. D. Santos, Dual-output DC-DC Buck converters with bidirectional and unidirectional Characteristics, IET Transactions on Power electronics, 6(5), 999–1009, (2013).
[18] M. S. Ebrahim, A. M. Sharaf, A. M. Atallah, and A. S. Emareh, An Efficient Controller for Standalone Hybrid-PV Powered System, Turkish Journal of Electromechanics and Energy, 2(1), (2017).
[19] M. A. El-Sharkawi, Fundamentals of Electric Drives, CI-Engineering, (2.Edition), 68-73, (2000).
[20] N. Mohan, Converters, Applications, and Design, John Wiley and sons Inc., (2. Edition), 161-200, (1995).
[21] Q. Leu, J. W. Jung, T. D. Do, E. K. Kim, H. H. Choi, Adaptive PID Speed Control Design for Permanent Magnet Synchronous Motor Drives, IEEE Transaction on Power Electronics, 30(2), 900-908, (2015).

Biographies

Ilyass Abdillahi Aden was born in Djibouti. He received his University Diploma of Technology in Industrial Engineering and Maintenance, and B.Sc applied in industrial maintenance from University of Djibouti, in 2013 and 2014 respectively. He is currently graduate student pursuing M.Sc. degree in the Department of Electrical and Electronics Engineering in KTU, Trabzon. His research interests include power electronics and renewable energy.

E-mail: ilyaden1992@gmail.com.

Hakan Kahveci was born in Kırşehir, Turkey. He received his B.Sc degree in Electrical Engineering and Ph.D degree from Karadeniz Technical University (KTU), Turkey, in 2006 and 2013, respectively. He is currently an assistant professor in Electrical and Electronics Engineering Department at KTU. He has been a member of the Chamber of Electrical Engineers in Turkey. He works on electrical machine control systems and power electronics.

E-mail: hknkahveci@ktu.edu.tr

Mustafa Ergin Şahin was born in, 1978 in Trabzon, Turkey. He received his B.Sc. degree in Electrical & Electronics Engineering from Karadeniz Technical University (KTU), M.Sc. degree from Gazi University in Ankara and Ph.D. degree from KTU, Trabzon, Turkey, in 2002 and 2006, 2014, respectively. He is currently an assistant professor in Electrical and Electronics Engineering Department at RTE University. He was worked at different projects on low voltage power systems and relay manufacturer for power systems. He is an active reviewer for scientific journals in the field. He is also member of the Chamber of Electrical Engineers in Turkey. His main research interests are power electronics and utilization of renewable energy.

E-mail: mustafaerginsahin@yahoo.com